JOURNAL OF SPACECRAFT AND ROCKETS
Vol. 37, No. 4, July–August 2000

Space Environment Effects on Damping of Polymer Matrix Carbon Fiber Composites

Thomas F. Klein III* and George A. Lesieutre†
Pennsylvania State University, University Park, Pennsylvania 16802

The effects of the low-Earth-orbit environment on the mechanical properties of some carbon-reinforced polymer matrix composites are reported. Material damping loss factors and glass transition temperatures of control and flight specimens were measured. Flight specimens were attached to the leading edge of the Long Duration Exposure Facility, and control specimens were maintained at the NASA Marshall Space Flight Center. Changes in the glass transition temperatures and damping were due to combined exposure to 1) atomic oxygen, 2) UV radiation, and 3) thermal cycling. High atomic oxygen exposure during the final year of the Long Duration Exposure Facility flight, however, eroded away much of the material that would have been affected by UV radiation. The glass transition temperatures of the flight samples were slightly greater than those of the controls, whereas the material loss factors were nearly the same. From a practical point of view, these changes were not very significant. However, the relaxation data presented herein may be useful for understanding the details of the effects of the space environment on composite materials and may aid researchers in developing composites that maintain their properties for extended periods in the harsh environment of low Earth orbit.

Nomenclature

c_i = peak value of distribution function for ith process
c_0 = peak value of distribution function
E_R = relaxed (low-frequency, high-temperature) storage modulus, Pa, psi
E_U = unrelaxed (high-frequency, low-temperature) storage modulus, Pa, psi
E^* = complex modulus, Pa, psi
E' = storage modulus, Pa, psi
E'' = loss modulus, Pa, psi
$F(z)$ = Fuoss–Kirkwood distribution
R = universal gas constant
T = temperature, °C
$T_{E''}$ = glass transition temperature (loss modulus peak), °C
T_f = glass transition temperature (storage modulus dropoff), °C
T_m = glass transition temperature (storage modulus midpoint), °C
T_p = temperature at a peak
T_η = glass transition temperature (loss factor peak), °C
w = frequency, rad/s
z = inverse temperature, $1/T$
z_i = inverse peak temperature for ith process
z_0 = inverse temperature at which distribution is centered
α = inverse of peak width
α_i = inverse of peak width for ith process
Δ = relaxation strength
ΔH = activation energy of a relaxation process, kcal/mol
η = loss factor
$\eta_{\max}$ = peak loss factor
τ = relaxation time
τ_ε = relaxation time at constant strain
τ_0 = characteristic jump time

Received 18 March 1998; revision received 28 February 2000; accepted for publication 29 February 2000.

*Graduate Research Assistant, Aerospace Engineering; currently Aerospace Engineer, Hughes Space and Communication, Redondo Beach, CA 90278. Member AIAA.

†Professor, Department of Aerospace Engineering, 233 Hammond Building. Associate Fellow AIAA.

Introduction

IN 1990, NASA astronauts retrieved the Long Duration Exposure Facility (LDEF) from low Earth orbit (LEO) after the LDEF had spent 69 months in space. This satellite was a large platform on which various materials having possible future spacecraft applications were exposed to the environment of space. In particular, several experiments on the spacecraft investigated the effects of 1) atomic oxygen, 2) UV radiation, 3) thermal cycling, and 4) vacuum on polymer matrix composites.

Preliminary findings[1] showed that atomic oxygen (AO) exposure eroded both the polymer matrix and fiber reinforcing materials along the leading face of the spacecraft (normal to the velocity vector), which lead to a reduction in mechanical properties. Microcracking was also observed in multidirectional carbon fiber reinforced composites, possibly due to thermal cycling.[2] UV radiation affected only a thin outer layer of the matrix materials on the trailing face composites, resulting in discoloration.[1] No UV effect was detected on the leading face specimens, probably because of the significant AO erosion.

Some analyses were performed to quantify the effects of the space environment on the glass transition temperatures of some of the polymer matrix composites. George[3] observed little or no change between the glass transition temperatures of control and flight carbon reinforced composites. Similarly, Young et al.[4] found only a slight increase in the glass transition temperatures of the LDEF samples compared to those of the control samples. However, there was no direct analysis of material loss factors to determine changes in the damping characteristics of the composite specimens.

The present research addressed the combined effects of AO, UV radiation, and thermal cycling in LEO on the glass transition temperatures and loss factors of carbon fiber reinforced polymer matrix composites. The objectives of this study were to verify the results of previous studies of glass transition temperatures and to provide additional data on loss factors that will enable researchers to develop composites that can better withstand long term exposure to the space environment.

Theory

Glass Transition Temperature

In American Society for Testing and Materials Standard E 1142, a glass transition is defined as the reversible change in an amorphous material from a hard and relatively brittle condition to a viscous or rubbery one.[5] There is some ambiguity, however, in the definition of the temperature at which this glass transition occurs in polymers. In some cases, the temperature at which the magnitude of the storage

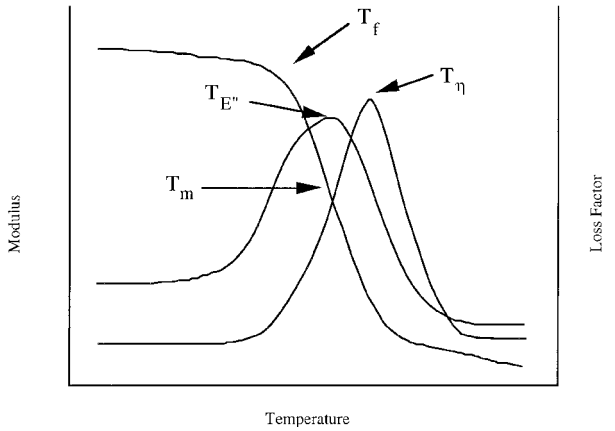

Fig. 1 Storage modulus, loss modulus, and loss factor as functions of temperature.

modulus begins to drop off significantly, T_f, is defined as the glass transition temperature. In other cases, the midpoint of the glass transition T_m is selected as the glass transition temperature.

With the use of data recorded by a dynamic mechanical analyzer (DMA), the glass transition temperature is often also selected at either the peak value of the loss modulus or at the peak in the loss factor, as illustrated in Fig. 1. The peak value of the loss modulus $T_{E''}$ is more closely associated with the onset of the glass transition T_f. Similarly, the peak value of the loss factor T_η more closely corresponds to the midpoint of the glass transition T_m (Ref. 6). Because many polymer matrix composites are used as structural members, it is more practical to define the glass transition as the temperature at which the storage modulus begins to drop off rather than at the midpoint of the transition.

Material Loss Factor

Material loss factor was the other characteristic of the composite specimens studied. The loss factor is a property of anelastic solids, materials that exhibit time dependence, or damping, in their stress–strain relationship. In dynamic testing of anelastic materials, a sinusoidal stress is often applied to the specimen. The complex modulus of a linear material E^* can be determined from the forced harmonic stress–strain behavior and can be expressed in terms of a real and an imaginary part:

$$E^* = E' + iE'' \tag{1}$$

The material loss factor η is a parameter that relates the loss modulus to the storage modulus as shown in Eq. (2). This loss factor is one measure of the inherent damping of the material and is directly related to the phase difference between stress and strain in forced harmonic reponse:

$$\eta = E''/E' \tag{2}$$

The storage and loss moduli for a standard anelastic solid are frequency- and temperature-dependent, and are sometimes expressed in terms of a relaxation strength Δ and a characteristic relaxation time at constant strain τ_ε. The quantity τ_ε determines the time to $1/e$ of completion of a stress relaxation process.[7] The relaxation strength is a dimensionless quantity that relates the unrelaxed (short-time, high-frequency, low-temperature) modulus E_U and its relaxed (long-time, low-frequency, high-temperature) modulus E_R as shown in Eq. (3):

$$E_U = E_R(1 + \Delta) \tag{3}$$

The frequency-dependent relations for the storage and loss moduli of a material having a single relaxation process may be expressed as follows:

$$E'(\omega) = E_R\left(1 + \Delta\frac{\omega^2\tau_\varepsilon^2}{1 + \omega^2\tau_\varepsilon^2}\right) \tag{4}$$

$$E''(\omega) = E_R\Delta\left(\frac{\omega\tau_\varepsilon}{1 + \omega^2\tau_\varepsilon^2}\right) \tag{5}$$

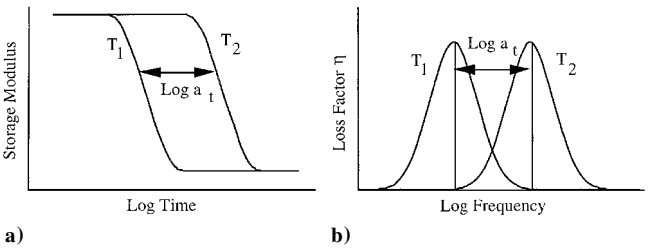

Fig. 2 Time–temperature superposition.

Note that the storage modulus has asymptotic values at low and high frequencies (highest at high frequencies) and that the loss modulus peaks at intermediate frequency corresponding to the characteristic time of the relaxation process (and approaches zero at the extremes). The material loss factor also exhibits a peak at an intermediate frequency, as shown in Eq. (6):

$$\eta(\omega) = \frac{\Delta\omega\tau_\varepsilon}{1 + (1 + \Delta)\omega^2\tau_\varepsilon^2} \tag{6}$$

Time–Temperature Superposition

The preceding relations are expressed as functions of frequency. However, when performing DMA testing, the complex modulus and loss factor is often measured over a range of temperatures at just a few frequencies. Such data can be related to frequency-dependent behavior through the time–temperature superposition principle. This principle states that the mechanical properties of an anelastic material at one temperature can be related to those at another temperature by a change in the time scale only.[8] In effect, the time constant associated with a relaxation process depends on temperature. In dynamic mechanical analyses, this principle explains shifts in the storage modulus and loss factor, as shown in Figs. 2a and 2b. In Figs. 2a and 2b, the curves are shifted by a time factor α_t only.

One possible relationship between time and temperature is given by the classical Arrhenius equation

$$\tau = \tau_0 e^{\Delta H/RT} \tag{7}$$

In Eq. (7), τ is a relaxation time, ΔH is the activation energy of a relaxation process, and R is the universal gas constant. In DMA testing, the material loss factor often exhibits peaks associated with different physical relaxation processes; an individual peak might be centered at a temperature T_p. (For a standard anelastic solid, the temperature at the peak T_p is the same as T_η.) The frequency and time constant at a peak are related through the relationship $\ln\omega\tau = 0$ (Ref. 7). If the Arrhenius equation is multiplied by ω, it indicates a linear relationship between $\ln\omega\tau$ and the inverse of the absolute temperature:

$$\ln\omega\tau = \ln\omega\tau_0 + (\Delta H/R)(1/T) \tag{8}$$

Now, when we substitute the conditions at the peak ($\ln\omega\tau = 0$ and $T = T_p$), Eq. (8) becomes

$$\ln\omega = -\ln\tau_0 - (\Delta H/R)(1/T_p) \tag{9}$$

If a DMA test is carried out at multiple frequencies, a plot of $\ln\omega$ vs $1/T_p$ can be constructed. The slope of a linear regression fit to this data then provides an estimate of $\Delta H/R$, from which the activation energy of the relaxation process ΔH can be determined. Along with the activation energy, the constant τ_0 can be calculated from the y intercept of the line fit.

Experimental Procedure

Specimens and Space Environment

Two groups of specimens were characterized, a set of control samples and a set of flight samples. The control samples were stored at the NASA Marshall Space Flight Center, whereas the flight samples were a part of the LDEF experiment AO171, Solar Array Materials Passive LDEF Experiment (SAMPLE). The flight samples were

Table 1 Composite samples flown on experiment A0171

Composite materials[a]	Weave, deg	Nominal size, mm	Sample no.
HMF 322/P1700[b,c]	±45	267 × 25 × 1.47	C-4, F-18
HMS/934[d,e]	0	267 × 13 × 1.18	C-1, F-29
HMS/934[d,e]	90	203 × 25 × 1.07	C-5, F-9
P75S/934[e,f]	90	203 × 25 × 1.04	C-4, F-15
P75S/934[e,f]	0	267 × 25 × 1.04	C-4, F-23

[a] All prepregs by Fiberite.
[b] HMF 322 carbon fiber, Toray Industries, Inc., Tokyo, Japan.
[c] Udel P-1700 polysulfone, Union Carbide Corp., Danbury, CT.
[d] HMS carbon fiber, Courtaulds Advanced Materials, Sacramento, CA.
[e] 934 epoxy, Composites Div., Fiberite Corp., Winona, WI.
[f] P75S carbon fiber, Amoco Performance Products, Inc., Greenville, SC.

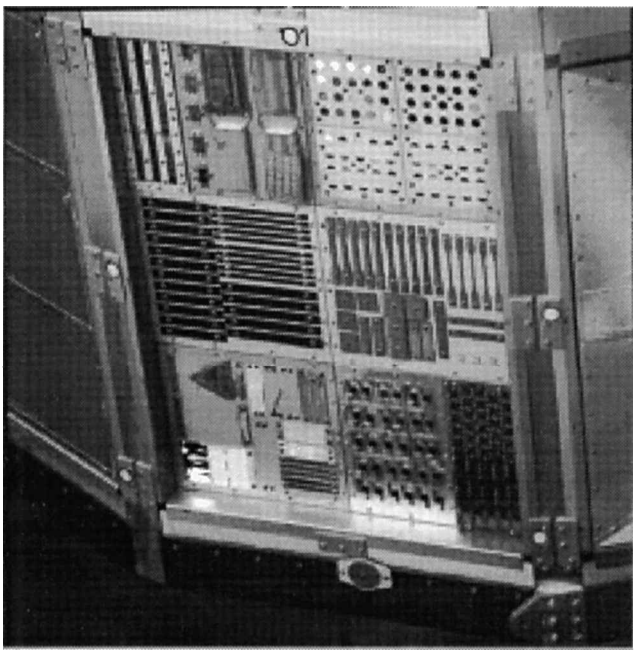

Fig. 3 On-orbit image of panel 8A showing experiment AO171.

mounted onto row 8, position A, at the end of the spacecraft facing outward into space. Figure 3 shows an on-orbit image of the panel onto which the group of flight composite samples was attached at the center left.

Table 1 lists the carbon reinforced polymer matrix composites that were flown as part of SAMPLE. Specimen data include the constituent materials and their manufacturers, fiber orientation, and nominal size. Three kinds of carbon fibers were used: HMF 322, HMS, and P75S, and two matrix materials were used: P1700 (a thermoplastic) and 934 (a thermoset). Before the launch of LDEF, all specimens were vacuum baked at 100°C and 10^{-6} torr for 3 h. This treatment minimized the amount of volatile material that would be outgassed in the high vacuum of space.

LDEF was placed into a near-circular orbit by the *Challenger* Shuttle on 7 April 1984, at an altitude of approximately 257 n mile and an inclination of 28.5 deg. Over time, the LDEF's altitude had decayed to 179 n mile, when it was retrieved on 12 January 1990. The flight samples on the 8A panel were oriented at approximately 38 deg to the incident AO exposure, resulting in the total space environmental exposure conditions listed in Table 2. About 54% of the total AO exposure occurred during the last six months of the LDEF flight, and approximately 77% during the final year in flight.[9]

Specimen Dynamic Properties

Researchers at the NASA Marshall Space Flight Center performed some initial analysis on the specimens after their retrieval from space. They used a profilometer to determine the thickness loss of the flight samples. Afterwards, they axially loaded the specimens in tension to failure and compared the results to those measured for the control samples. These specimens were characterized further in the present research.

Table 2 Experiment A0171 exposure conditions

Parameter	Value
Flight time	Approximately 69 months
High vacuum	10^{-6}–10^{-7} torr (estimated)
UV radiation	10,471 equivalent sun hours (ESH)
Proton fluence	10^{9} p^{+}/cm^2 (0.5–200 MeV)
Electron fluence	10^{12}–10^{18} e^{-}/cm^2 (0.05–3.0 MeV)
AO	6.93×10^{21} atoms/cm^2
Micrometeroids/space debris	2–5 impacts per 25 cm^2, <1 mm diameter (2–7 impacts per composite)
Thermal cycles	≈32,000 cycles (temperature unknown)

Table 3 Dimensions of DMA samples[a]

Specimen	Thickness, mm	Width, mm
HMF 322/P1700		
Control	1.52	11.73
Flight	1.47	11.15
HMS/934 0 deg		
Control	1.12	7.04
Flight	0.89	5.87
HMS/934 90 deg		
Control	1.09	11.32
Flight	0.99	11.26
P75S/934 0 deg		
Control	1.09	6.79
Flight	0.94	5.18
P75S/934 90 deg		
Flight	0.99	11.53

[a] Length is 20.00 mm.

Before running the DMA as part of the present research, all of the LDEF specimens were sized to fit into the sample holder. Table 3 lists the dimensions of the samples used for these measurements. The erosive effect of AO on the epoxy resin composites is readily seen by comparing the thicknesses of the control and flight samples. In the case of the HMS/934 0-deg specimens, there was a 0.23-mm (approximately 20%) reduction, whereas for the polysulfone matrix composites there was only a loss of 0.05 mm (approximately 3%).

Once each sample was prepared, both ends were clamped in a double cantilever condition within a Seiko DMS110 bending module. The temperature profile was set in a ramp mode with a low heating rate of 2.0°C/min with a maximum oven temperature of 350°C. Next, a set of five test frequencies was selected. A frequency setting of 1 Hz was selected so that the resulting data could be used to determine the glass transition temperatures, as recommended in Ref. 5. The other four frequencies selected were 0.2, 5, 10, and 20 Hz. The data collected at these five test frequencies were used to establish the material loss factors and time–temperature shifts. After the desired program was set up and executed, the same experimental procedure was followed for all nine test specimens.

Glass transition temperatures were determined from plots of loss modulus, loss factor, or storage modulus vs temperature, at a fixed frequency (nominally 1 Hz). The temperature at which the peak loss modulus is observed defines $T_{E''}$, the temperature at which the peak loss factor is observed defines T_{η}, and the temperature at which the storage modulus begins to drop off defines T_f.

In studies of material loss factor, loss data were plotted vs inverse temperature. After satisfactory agreement with previous data[1] was verified, the influence of fiber orientation was considered. This comparison illuminates the relative effects of the matrix and fiber materials.

The composite loss factor data generally exhibit broad and/or multiple peaks when plotted vs inverse temperature and, furthermore, the locations of these peaks shift with frequency. The experimental loss factor data were curve fit with a series of Fuoss–Kirkwood distribution functions, using the Igor™ software package.[10] The Fuoss–Kirkwood distribution is a hyperbolic secant function, as shown in Eq. (10):

$$F(z) = c_0 \operatorname{sech}[\alpha(z - z_0)] \tag{10}$$

In Eq. (10), the coefficient c_0 is the peak value of the distribution function centered at z_0, and the inverse of α defines the width of the peak. Because the composite specimens studied herein exhibited multiple peaks in loss factor, Eq. (10) was modified to be a sum of three distribution functions as follows, with each peak assumed to be associated with a different relaxation process:

$$F(z) = \sum_{i=1}^{3} c_i \operatorname{sech}[\alpha_i(z - z_i)] \tag{11}$$

From the curve fits, the peak magnitudes c_i, the widths $(1/\alpha_i)$, and the temperatures of the peak centers $T_{pi} = 1/z_i$ were determined. With these parameters in hand, the test frequency was plotted against the inverse temperature of the peak temperatures for the second and third peaks, and Eq. (9) was used to determine the activation energies of the associated relaxation processes. Changes in a polymeric material due to exposure to the space environment might be detected as changes in the activation energy of a particular microstructural loss mechanism.

Results

Glass Transition Temperatures

Table 4 summarizes the results from the 1-Hz dynamic mechanical analyses of the glass transition temperature. The $T_{E''}$ and T_η transition temperatures listed in Table 4 are the temperatures at the overall peaks in the loss modulus and loss factor, respectively. The dropoff glass transition temperatures T_f have an uncertainty of about ±3.0°C, whereas $T_{E''}$ and T_η have uncertainties of approximately ±1.0°C.

When only the dropoff glass transition temperatures in Table 4 are considered, the difference between the control and flight specimens of the same matrix type and fiber orientation is on the order of 2–6°C. For example, the transition temperature of the HMS/934 0-deg control sample is 190.5°C, whereas the corresponding temperature for the flight sample is 196.5°C. The other 934 matrix specimens exhibited similar small increases in the transition temperature from the control sample to the flight. On the other hand, the glass transition temperatures measured for the polysulfone matrix specimens decreased by about 1.0°C.

Overall, there was about a 3% change in the transition temperatures between the control and flight specimens, a value that is not much larger than the associated experimental uncertainties. In addition, from the standpoint of thermally stable material stiffness, this change in the transition temperature is minimal. The exposure to the LEO space environment did not significantly change the glass transition temperatures of these carbon reinforced polymer composites.

Other composite specimens flown elsewhere on the LDEF had the same epoxy and polysulfone matrix systems. Young et al.[4] examined P1700/C6000 polysulfone/carbon composites and found that the glass transition temperature of the control samples was 167°C, whereas that of the exposed flight specimens was 170°C. This reinforces the conclusion that there was at most a small change in the transition temperature of composites on the leading face of the LDEF. In addition, George[3] studied specimens that contained either the 934 epoxy or the P1700 polysulfone matrix systems. Both composite types were reinforced by T300 carbon fibers. The transition temperature of the 934 matrix control sample was 191°C, and for the flight sample it was 189°C. For the polysulfone composites, the T_g of the flight sample was 190°C. For the control specimen, however, George believes that he recorded an inaccurate transition temperature of 167°C. George generally found only a small change in transition temperatures. The differences between the glass transition temperatures of the composite specimens tested in this research and those examined by Young et al.[4] and George[3] are perhaps due to different fabrication conditions of the composites and to different types of carbon reinforcement.

Before testing, it was expected that the glass transition temperatures of the three 934 epoxy control specimens would be very similar because the glass transition process in polymer matrix composites is a matrix-dominated phenomenon. However, as shown in Table 4, the transition temperatures of the HMS carbon reinforced composites are nearly 15°C higher than those of the P75S 0-deg carbon reinforced samples. These changes could be a result of the different types of fiber reinforcement or, more likely, the result of slightly different cure cycles. If Fiberite used the same cure process for all of the 934 epoxy matrix composites, the glass transition temperatures should have been nearly the same regardless of the reinforcement type.

Table 4 Glass transition temperatures from 1-Hz test

Specimen	T_f, °C ± 3.0°C	$T_{E''}$, °C ± 1.0°C	T_η, °C ± 1.0°C
HMF 322/P1700			
Control	177.5	183.7	191.2
Flight	176.5	181.2	193.3
HMS/934 0 deg			
Control	190.5	214.4	239.3
Flight	196.5	222.7	228.7
HMS/934 90 deg			
Control	185.5	195.7	224.9
Flight	189.0	197.8	227.1
P75S/934 0 deg			
Control	176.0	190.3	224.0
Flight	177.5	194.1	218.5
P75S/934 90 deg			
Flight	197.0	217.3	231.2

Material Loss Factors

Figures 4–9 show the material loss factor data for the four HMS/934 and the two P75S/934 0-deg specimens. In Figs. 4–9, the loss factors for the five test frequencies are plotted as functions of inverse temperature.

As mentioned earlier, the SAMPLE specimens were loaded in tension to failure. It was not known if this damage would affect the results of subsequent dynamic mechanical analysis of the remaining parts. Thus, the first comparison of the material loss factor was with sample data from George and Hill.[1] Reference 1 includes a sample plot of the loss factor as a function of temperature for a T300/934 carbon/epoxy specimen that was attached to the LDEF. The overall

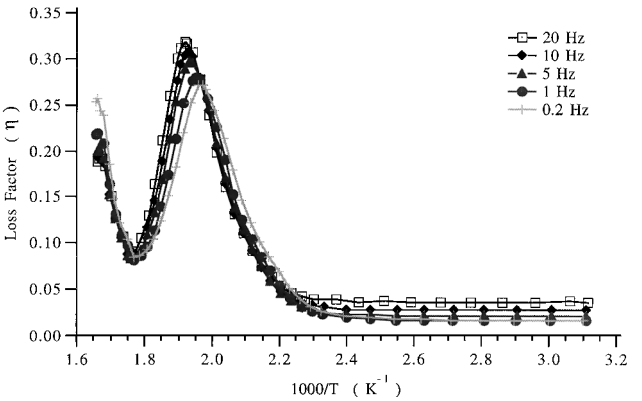

Fig. 4 Material loss factor data for HMS/934 0-deg control specimen.

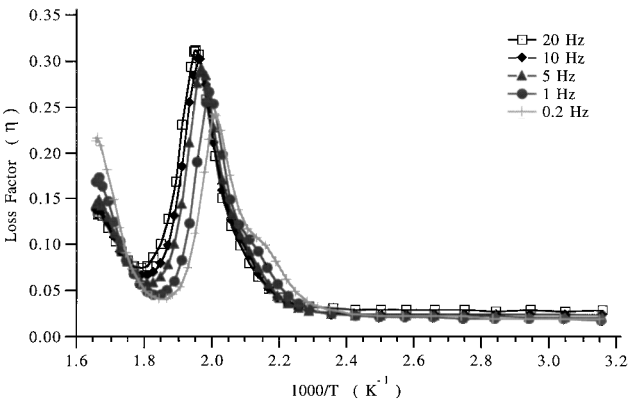

Fig. 5 Material loss factor data for HMS/934 0-deg flight specimen.

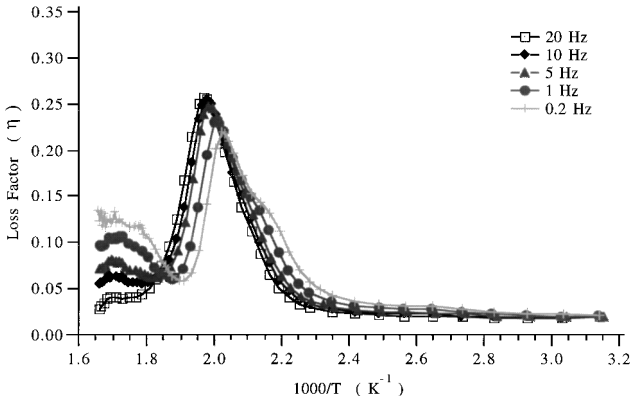

Fig. 6 Material loss factor data for HMS/934 90-deg control specimen.

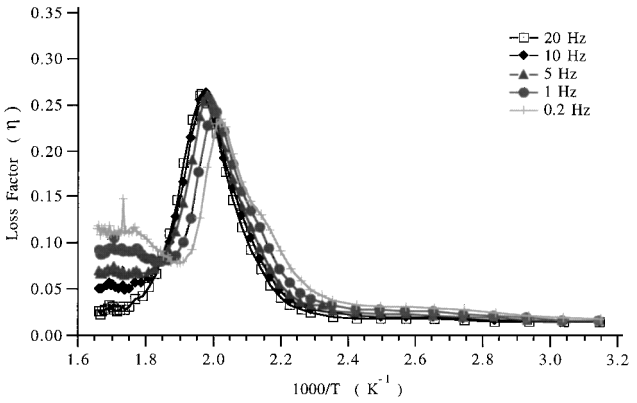

Fig. 7 Material loss factor data for HMS/934 90-deg flight specimen.

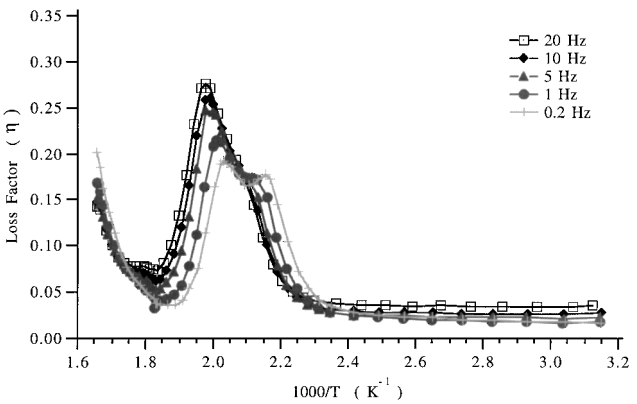

Fig. 8 Material loss factor data for P75S/934 0-deg control specimen.

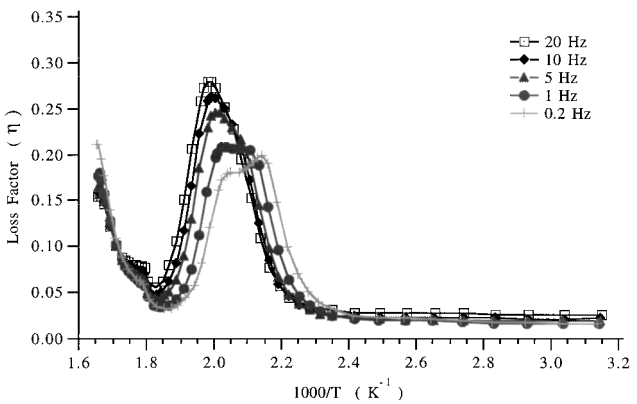

Fig. 9 Material loss factor data for P75S/934 0-deg flight specimen.

Table 5 Overall loss factor peak data for 934 epoxy specimens

Specimen	T_η, °C	η_{max}
HMS/934 0 deg		
Control	239.3	0.279
Flight	228.7	0.266
HMS/934 90 deg		
Control	224.9	0.214
Flight	227.1	0.208
P75S/934 0 deg		
Control	224.0	0.231
Flight	218.5	0.245
P75S/934 90 deg		
Flight	231.2	0.326

peak value η_{max} was approximately 0.25 at a temperature of about 220°C. These values compare favorably with data from the present study. As shown in Table 5, the temperatures at the overall loss factor peak of the SAMPLE specimens having the same epoxy resin as studied in Ref. 1 are in the same temperature range. In addition, the peak values at these temperatures are close to 0.25. From this comparison, the present DMA results are assumed acceptable.

The next general comparison made was based on fiber orientation. There is a clear difference between the data for the 0-deg fiber orientation samples and those for the 90-deg samples. Figure 5 shows the material loss factor data for the HMS/934 0-deg flight specimen. When these data are compared with those in Fig. 7 (for the HMS/934 90-deg flight sample), the pronounced peak on the left-hand side of the 0-deg specimen plot is not as well defined for the 90-deg specimen. As is generally known for continuous fiber reinforced composites, the fibers have a significant effect on the overall stiffness in the longitudinal direction, whereas they have a minor effect in the transverse direction. Similarly, any overall loss factor associated primarily with relaxation processes in the fibers would be more evident in the data from the 0-deg (longitudinal) specimens than in the data from the 90-deg (transverse) specimens, as seen here.

The peak on the left-hand side of the loss factor plots may be associated with a relaxation process within the carbon fibers. This effect is observed at temperatures above 300°C, approximately 100°C higher than the (matrix-dominated) glass transition temperature T_f. On the other hand, this peak could be related to transverse shear of the matrix accentuated by the high longitudinal composite modulus.

When we compare the data between the control and flight samples for a given set of constituents and fiber orientations, some differences may be noted. In the case of the P75S/934 0-deg control and flight specimens, a discernible change is observed in the loss factor. Figures 8 and 9 show the material loss factor vs inverse temperature for the P75S/934 control and flight specimens, respectively. For the lowest two test frequencies, there is a substantial change in the height of the right-hand side peak, centered between 2.1 and 2.2 on the horizontal axis. For the 0.2-Hz test frequency, the right-hand peak is higher than the center peak for the flight sample when compared with the peaks for the control sample. This suggests that extended exposure to the LEO environment resulted in a detectable change in material damping characteristics. Also, for the HMS/934 specimens, the right-hand peaks of the flight specimens (Figs. 5 and 7) are slightly more pronounced than those of the control specimens (Figs. 4 and 6). This again suggests that extended exposure to the LEO environment affected the material damping properties.

Activation Energies

The effects of different test frequencies on the material loss factor are apparent in the data. For example, in Fig. 9 the center of the overall peak is shifted to the left for increasing frequencies. This corresponds to an increase in the glass transition temperature T_η as the test frequency increases. Along with this shift, the height of the overall peak also increases with frequency. The small hump peak seems to decrease in height with an increase in frequency even though its center also appears to shift to the left at higher frequencies. (The shapes and sizes of individual peaks are discussed further in the following section on the curve fit results.) With regard to the

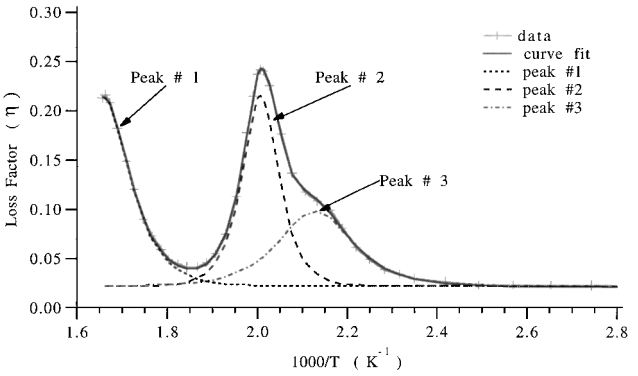

Fig. 10 Loss factor data and curve fit for HMS/934 0-deg flight specimen at 0.2 Hz.

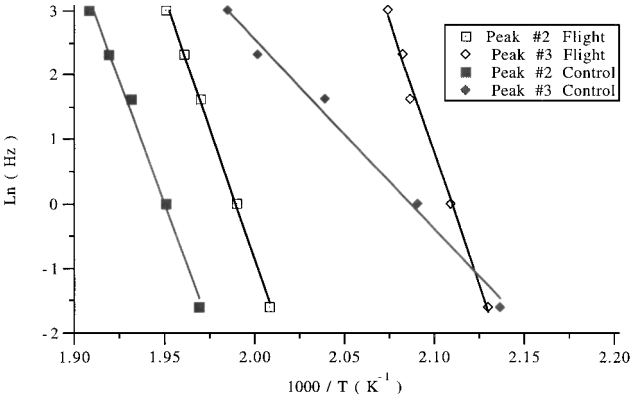

Fig. 11 Test frequency vs inverse peak temperature for the HMS/934 0-deg specimens.

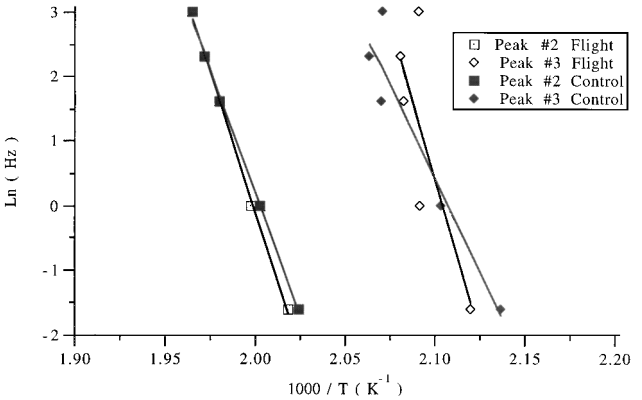

Fig. 12 Test frequency vs inverse peak temperature for the HMS/934 90-deg specimens.

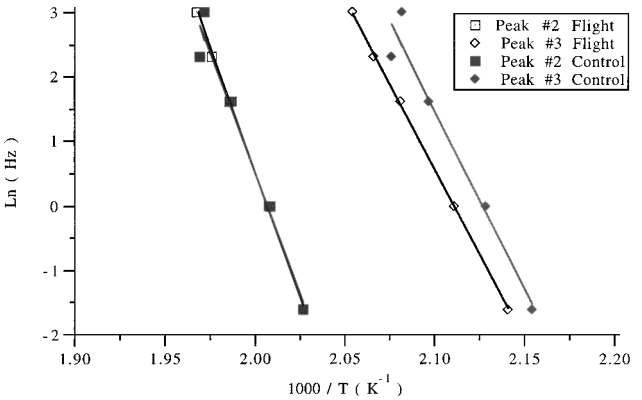

Fig. 13 Test frequency vs inverse peak temperature for the P75S/934 0-deg specimens.

peak on the left-hand side of the loss factor plots, no conclusions can be drawn about changes in the height nor in the position of its center because there are not enough data to complete the peak for any of the samples at temperatures over 330°C.

Figure 10 shows an example of the curve fit to the 0.2-Hz data for HMS/934 0-deg flight specimen. There is excellent agreement between the three-term Fuoss–Kirkwood fit and the data, with the maximum difference being less than 4.0%. Also shown are the three individual peak functions that correspond to different damping mechanisms. The curve fit procedure resolved the predominant peak and the hump into two distinct peaks that overlap each other in the region between 1.9 and 2.2 of the horizontal axis.

The temperatures at the centers of the second (dominant) peaks increased with frequency for all specimens. The height and the width of these peaks also generally increase with test frequency. However, the HMS/934 0-deg control specimen is the exception to this rule. For this specimen, the height and width decrease with increasing frequency. The hump peaks of both of the HMS/934 90-deg specimens followed the same trends as the HMS/934 0-deg flight sample. On the other hand, these tendencies were not found in the HMS/934 0-deg control and either of the P75S/934 samples.

There is no consistent change with frequency between the specimens in the temperature at the center of the first peak. The same holds true for the widths of the first peaks. In the case of the first peak, several of the temperatures determined by the curve fits are greater than the highest experimental temperature and also have high uncertainties. This is especially true of the two P75S/934 0-deg specimens for which the peak temperatures, between 345 and 475°C, have uncertainties between 10 and 25°C. The explanation for these extremely high temperatures and for the inconsistent trends in the curve fit parameters for the first peak is the lack of data for temperatures above 330°C. Without these data, the shape and size of this peak can not be accurately defined, nor can the corresponding activation energies be accurately calculated. Thus, the only statement that can be confidently made about the first peak is that it may be associated with a relaxation process within the carbon fibers.

The parameters from the curve fits for the third peak did not exhibit an obvious trend. The lack of a trend is most likely due to the lack of uniqueness in the curve fits. The curve fitting software assigns parameters to peaks that are extremely close together. Thus, instead of one peak matching the majority of the overall central peak, the curve fitting software assigned more balanced parameters to both the second and third peaks. If a different set of initial guesses was chosen, the resulting curve fit parameters may have been different. An attempt was made to constrain the magnitudes of either the heights or the widths for the peaks to see if the resulting curve fit parameters could be encouraged to follow a more consistent trend. However, this did not happen: the accuracy of the fits decreased.

With parameters obtained from the curve fits, activation energies were determined for the second and third peaks of each specimen. Figures 11 and 12 are for the HMS/934 0 and 90-deg samples, respectively, whereas Fig. 13 is for the P75S/934 0-deg specimens. In Figs. 11–13, the effect of the space environment on material properties is apparent. For the HMS/934 90-deg and P75S/934 0-deg specimens, there is almost no shift in the line fit for the second peaks, unlike the HMS/934 0-deg data. For the third peaks of the HMS/934 samples, the slopes of the line fits are greater for the flight samples. Again, this may possibly be a result of the nonuniqueness of the curve fit parameters in light of experimental uncertainties.

Table 6 lists the activation energies estimated from the plots of test frequency vs inverse peak temperature for the second and third loss factor peaks of the 934 epoxy specimens. There is an increase of about 7% in the activation energies of the second peaks of the flight specimens relative to those of the control specimens. This increase in activation energy may be a result of greater crosslink density because of 1) UV radiation exposure, 2) thermal cycling, or 3) some combination of the two effects.

For the third peaks, the activation energies of the specimens varied greatly. It seems unlikely that these variations are the result of a space environmental effect. The variations are most likely due to the assignment of curve fit parameters to a pair of peaks that are in

Table 6 Activation energies for 934 epoxy specimens

Specimen	Activation energy for peak 2, kcal/mol	Activation energy for peak 3, kcal/mol
HMS/934 0 deg		
Control	151	58
Flight	160	161
HMS/934 90 deg		
Control	151	113
Flight	172	190
P75S/934 0 deg		
Control	146	109
Flight	153	105
P75S/934 90 deg		
Flight	153	64

close proximity. Also note that, whereas the parameters of the second peak affect the parameters of the third peak, the reverse is also true. The observed changes in activation energies between the control and flight specimens are affected by the accuracies of the line fit slopes. If more frequencies had been used during the DMA tests, the uncertainties in the activation energies would likely be lower.

Conclusions

The effects of the LEO environment on the glass transition temperatures and loss factors of carbon reinforced polymer composites were studied. Composite specimens were attached to the leading face of the LDEF where they were continuously exposed to a high fluence of incident AO. Using a dynamic mechanical analyzer, the complex moduli of the specimens were experimentally determined as a function of temperature and frequency. The glass transition temperatures of the flight specimens were slightly higher than those of the control specimens. From a practical point of view, this change was not significant.

The material loss factor data were analyzed to determine the effects of the environment on the damping characteristics of the composites. The data were curve fitted with a series of Fuoss–Kirkwood distribution functions. These fits matched the overall data for different specimens and frequencies very accurately. The predominant second peak followed the expected trends associated with the time–temperature superposition principle. The parameters of the other two peaks, however, did not follow the same trends. In the case of the first peak, inconsistent trends were believed to be the result of data insufficient to define fully the peak associated with a relaxation process within the carbon fibers. For the third peak, the inconsistent trends were believed to be the result of nonunique curve fits. For the dominant second peak, the activation energies of relaxation processes in the flight specimens were slightly greater than the activation energies for the corresponding processes in the control specimens.

The small changes in the damping characteristics of the flight samples are similar to the changes in the glass transition temperatures: there were negligible changes in the properties of the leading-edge flight composites due to environmental effects other than AO erosion. Because UV radiation only affects a thin layer of the surfaces of the composites, it is believed that the incident AO eroded away most of the UV-damaged surface as the damage was occurring. This is especially true for the last six months of exposure, during which time over half of the total amount of AO exposure occurred. Thus, at these altitudes, AO is the dominant space environment effect on the mechanical properties of composite specimens attached to the leading edge of the LDEF. Other researchers have found that it is possible to significantly reduce the erosion of leading-edge composites by adding thin coatings of oxygen-resistant materials like aluminum or by using advanced resin systems that themselves are highly resistant to AO.

In conclusion, the objective of this research was to determine the effect of the space environment on the glass transition temperatures and material loss factors of some carbon reinforced polymer composites. Although the results suggest that there were only small changes in the material properties themselves, the information provided here may enable other researchers to develop polymer composites that can better withstand the environmental effects of LEO for long periods of time.

Acknowledgments

Miria Finckenor of the NASA Marshall Space Flight Center graciously provided the LDEF samples. James Runt of the Polymer Science Department at Pennsylvania State University allowed the use of his dynamic mechanical analyzer and assisted in establishing the test method. Special thanks also to Anthony Amos for his advice and comments.

References

[1]George, P. E., and Hill, S. G., "Results from Analysis of Boeing Composite Specimens Flown on LDEF Experiment M0003," *LDEF-69 Months in Space: First Post-Retrieval Symposium*, NASA CP-3134, 1992, p. 1115.

[2]Jang, B. Z., Bianchi, J., Liu, Y. M., and Chang, C. P., "Space Environmental Effects on Polymer Composites: Research Needs and Opportunities," *LDEF Materials Results for Spacecraft Applications*, NASA CP-3257, 1994, p. 319.

[3]George, P. E., "Space Environmental Effects on LDEF Low Earth Orbit Exposed Graphite Reinforced Polymer Matrix Composites," *LDEF Materials Workshop '91*, NASA CP-3162, 1991, p. 543.

[4]Young, P. R., Slemp, W. S., and Stein, B. A., "Performance of Selected Polymeric Materials on LDEF," *LDEF Materials Results for Spacecraft Applications*, NASA CP-3257, 1994, 1992, p. 125.

[5]Seyler, R. J., "Opening Discussion," *Assignment of the Glass Transition*, STP 1249, American Society for Testing and Materials, West Conshohocken, PA, 1994, p. 1.

[6]Chartoff, R. P., Weissman, P. T., and Sircar, A., "The Application of Dynamic Mechanical Methods to Tg Determination in Polymers: An Overview," *Assignment of the Glass Transition*, STP 1249, American Society for Testing and Materials, West Conshohocken, PA, 1994, pp. 88–107.

[7]Nowick, A. S., and Berry, B. S., *Anelastic Relaxation in Crystalline Solids*, Academic, New York, 1972, pp. 49, 50.

[8]Ward, I. M., *Mechanical Properties of Solid Polymers*, 2nd ed., Wiley, New York, 1983.

[9]Bourassa, R. J., Gillis, J. R., and Rousslang, K. W., "Atomic Oxygen and Ultraviolet Radiation Mission Total Exposures for LDEF Experiments," *LDEF-69 Months in Space: First Post-Retrieval Symposium*, NASA CP-3134, 1992, p. 643.

[10]*Igor Graphic and Data Analysis User's Manual*, WaveMetrics, Inc., Lake Oswego, OR, 1991, pp. 521–547.

I. D. Boyd
Associate Editor